Molecular Dynamics Study of a Polymeric Reverse Osmosis Membrane

Edward Harder,[†] D. Eric Walters,[‡] Yaroslav D. Bodnar,[§] Ron S. Faibish,*[,§] and Benoît Roux*[,†]

Department of Biochemistry and Molecular Biology, Center for Integrative Science, University of Chicago, Illinois, 60637, Chicago Medical School, Rosalind Franklin University of Medicine and Science, North Chicago, Illinois, 60064, and Nuclear Engineering Division, Argonne National Laboratory, Argonne, Illinois, 60439

Received: March 25, 2009; Revised Manuscript Received: May 12, 2009

Molecular dynamics (MD) simulations are used to investigate the properties of an atomic model of an aromatic polyamide reverse osmosis membrane. The monomers forming the polymeric membrane are cross-linked progressively on the basis of a heuristic distance criterion during MD simulations until the system interconnectivity reaches completion. Equilibrium MD simulations of the hydrated membrane are then used to determine the density and diffusivity of water within the membrane. Given a 3 MPa pressure differential and a 0.125 μm width membrane, the simulated water flux is calculated to be 1.4×10^{-6} m/s, which is in fair agreement with an experimental flux measurement of 7.7×10^{-6} m/s.

Downloaded by UNIV OF CHICAGO on August 27, 2009 | http://pubs.acs.org
Publication Date (Web): July 8, 2009 | doi: 10.1021/jp902715f

1. Introduction

The application of membranes in material separation is increasingly used in a wide range of process applications in the petrochemical, pharmaceutical, food, biotech, pulp and paper production, and water treatment industries.[1,2] One important example is the utilization of semipermeable membranes to produce fresh water, suitable for human consumption and irrigation, through the desalination of seawater. This process, called reverse osmosis (RO), exploits a differential permeability that favors water over solute impurities (salt ions), by passing the mixture under a significant pressure gradient (~5 MPa for typical seawater salt concentrations at temperatures between 25 and 30 °C). To improve process efficiency, the design of new membrane materials should aim to maximize water flux at a particular pressure gradient while maintaining a high salt rejection level. Toward this goal, it is imperative that a detailed understanding be established that relates the atomic structure of these membranes to the mechanism of solute permeation.

Polymeric RO membranes, based on aromatic polyamide thin-film composites (TFCs), are currently the most widely used for the desalination and purification of seawater and brackish water. RO membranes typically consist of a polyamide separation layer that is formed by interfacial polymerization on a microporous polysulfone support. An example of such a membrane is the Dow FILMTEC FT30 which is composed of *m*-phenylenediamine (MPD) and benzene 1,3,5-tricarboxylic acid chloride (TMC) monomers that react to form a densely cross-linked polymeric material.[3] Although the FT30 membrane is one of the simplest examples of polymeric RO membranes, it has a complex structure and morphology. The density of FT30 is highly nonuniform and has been characterized in the literature by positron annihilation lifetime spectroscopy (PALS).[4,5] The performance characteristics of TFC membranes are primarily determined by the transport properties of the polyamide separation layer, which depend on the microscopic physicochemical properties of these polymeric thin films. However, because of difficulties with the experimental characterization of polymeric materials, little is known about the detailed atomic structure and molecular mechanisms of water permeation and ion transport through these membranes.[6] Without further insight into these structural and mechanistic details, it is difficult to imagine how to alter the chemical structure of the monomers or the polymerization process to optimize the properties of TFC membranes.

One method that can advance our understanding of RO membranes is computational modeling and molecular dynamics (MD) simulation. Such models employ physical potential functions (i.e., molecular mechanics force fields) with atomic-level detail. MD simulations can provide essential details on the molecular mechanisms of water and solute transport through RO membranes that are not directly available via experiments. This may ultimately lead to significant improvement over current, state of the art, RO membrane technologies. MD has been used extensively to understand the transport mechanisms of gas-phase separations, such as the transport of CO_2, H_2, CH_4, N_2, and Xe through inorganic zeolite[7−13] and carbon molecular sieve membranes.[14,15] More recently, MD simulations have been used to study water transport using RO carbon nanotube membranes.[16,17]

The experimental information that is currently available is not sufficient to unambiguously build a complete and accurate three-dimensional all-atom model of the FT30 membrane that is suitable for MD simulations aimed at evaluating the transport properties and performance of this membrane. There is an unavoidable random aspect to the polymerization process used to make the membrane, and for this reason, its structure cannot be modeled as a well-ordered material. Whereas past efforts to model the atomic membrane structure of FT30 have employed methods that incorporate experimental elements into the design of the polymer,[18] we present a novel, heuristic, MD-based approach for producing an atomistic model of a typical thin-film polyamide RO membrane. The method allows for the polymerization of MPD and TMC monomers to form the polymeric thin-film material in a way that more realistically simulates the interfacial polymerization process used in RO synthesis. The MD simulations performed in this study take into

* E-mail: roux@uchicago.edu (B.R.) and rfaibish@anl.gov (R.S.F.).
[†] University of Chicago.
[‡] Rosalind Franklin University of Medicine and Science.
[§] Argonne National Laboratory.

10.1021/jp902715f CCC: $40.75 © 2009 American Chemical Society
Published on Web 07/08/2009

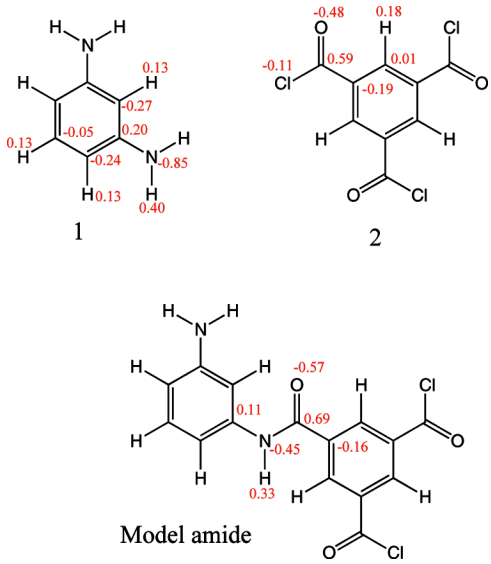

Figure 1. The generalized AMBER force field (GAFF) was used for MPD (meta-phenyldiamine, compound 1), TMC (benzene-1,3,5-tricarboxylic acid chloride, compound 2), and the amide linkage (bottom). The topology and parameters for the monomers and for a model benzene 1,3,5-tricarboxylic phenylamide (**3**) were generated with ANTECHAMBER 1.27 and with AM1-BCC partial charges. Atomic charges were averaged for symmetrically related atoms in each monomer. Chemical bonding of TMC and MPD involves the formation of an amide linkage between the amine and the carbonyl moieties.

account self-limiting phenomena, in which the polymeric material becomes sufficiently dense such that the polymerization reaction rate drastically decreases because of the inability of monomer molecules to diffuse inside the polymer network.[19] The goal of the proposed method is to employ physical interactions between molecules to produce an atomistic model that realistically reproduces the cross-linking frequency, degree of polymerization, and other physicochemical properties of such polymeric thin-film materials. By performing MD simulations of water permeation through the obtained FT30 polyamide membrane material, the diffusivity and permeability of water through the model membrane can then be calculated and compared with experimental values.

2. Membrane Model

Intermolecule interactions, in the polymeric system studied, are based on an atomistic resolution force field model. The nonbonded potential energy includes Coulombic interactions between partial atomic charges and a Lennard-Jones potential representing intermolecule repulsion and dispersion. Further details of this potential are provided in ref 20. Models for TMC, MPD, and the amide-bonded oligomer, 1,3,5-tricarboxylic phenylamide, were built using the generalized AMBER force field (GAFF).[21] The topology and parameters for the compounds were generated with ANTECHAMBER 1.27 and with AM1-BCC partial charges.[22,23] Atomic charges were averaged for symmetrically related atoms in each monomer. The chemical structure of the model compounds along with their partial charges is shown in Figure 1. Simulations that include explicit water molecules employ the TIP3P water model.[24]

An atomistic model of the RO membrane is built using a heuristic approach that uses molecular simulation of the monomers in vacuum, without explicit solvent, to drive the process of membrane polymerization. The goal is to assemble a system matching the experimental layer density of the FT30 membrane (1.38 g/cm^3) and water content level of 23 wt %.[25] First, 250 TMC and 250 MPD monomers are randomly positioned and oriented within a volume twice that of the target density (unit cell length = 61.3 Å). No water molecules are included in the initial assembly. The length of the unit cell is then subsequently reduced by 0.5 Å increments followed by energy minimization and 1000 steps of MD, until the target density is reached (unit cell length = 48.7 Å). The polymerization of the membrane from these constituent monomers follows a build-up procedure with several distinct stages that aims to expedite the polymerization process. The membrane construction and simulations were performed with the program CHARMM.[20]

As an initial step, denoted stage 0, a random configuration of all of the monomers was generated without steric clashes. In stage 1, an energy minimization followed by a short MD simulation is carried out from the stage 0 configuration, with the process of polymerization progressing through amide bond formation events interspersed at 1 ps intervals. The criterion used to add a new amide bond is based on an intermolecule distance determination. When the nitrogen of a free amine group approaches within 3.25 Å of the carbonyl carbon of a free acyl chloride group, a molecular topology transformation is performed that creates an amide bond; after approximately 1 ns of simulation time the distance criteria was relaxed to 3.5 Å. In the CHARMM program, the topological transformation is executed via a PATCH to the PSF, which is the data structure that contains the list of all covalent energy terms (bond, angles, dihedrals, etc.).[20] Through the PATCH command, the parameters associated with the individual functional groups shown in Figure 1 (top) are replaced by the parameters and bond topology associated with the amide-bonded compound (Figure 1, bottom). Simulations are conducted in periodic boundary conditions with bond formation restricted to molecule pairs that lie within the primary unit cell of the system.

When the time rate of change of polymerization in stage 1 falls to approximately zero, stage 2 begins. To encourage further association of unreacted functional groups, an additional intermolecule potential is introduced between the nearest amine and the acyl chloride groups. The additional potential has the following functional form,

$$U(r) = 0.0 \qquad 3.5\ \text{Å} < r$$

$$U(r) = 1.25(R - 3.5)^2 \qquad 3.5\ \text{Å} < r < 6.0\ \text{Å}$$

$$U(r) = 6.0(R - 4.75) \qquad r > 6.0\ \text{Å}$$

where the intermolecular distance r is between the nitrogen of an amine group and the carbonyl carbon of an acyl chloride group. The form of the restraint potential is chosen so as to provide a weak linear bias at larger intermolecule distances and a stronger (quadratic) attraction as the molecule pair approach. Simulation interspersed by polymerization events proceeds in much the same manner as in stage 1 with the additional potential energy discussed above.

The final stage (stage 3) of membrane polymerization follows when once again the time rate of change of bond formation drops to approximately zero. In this stage, free acyl chloride monomers are translated to positions near unreacted amine groups, and cycles of simulation with bond formation are repeated under the potential function used in stage 2. Finally, remaining free monomers are deleted from the system, giving the final membrane structure.

Downloaded by UNIV OF CHICAGO on August 27, 2009 | http://pubs.acs.org
Publication Date (Web): July 8, 2009 | doi: 10.1021/jp902715f

Downloaded by UNIV OF CHICAGO on August 27, 2009 | http://pubs.acs.org
Publication Date (Web): July 8, 2009 | doi: 10.1021/jp902715f

3. Simulation Details

All MD simulations were performed with the program CHARMM using a Verlet algorithm.[20,26] In the water-solvated membrane simulation, the temperature is controlled by a Nose-Hoover thermostat, and the pressure is controlled by an Andersen barostat.[26] The SHAKE algorithm is used to constrain covalent bonds to hydrogens to their equilibrium value.[26]

Periodic boundary conditions were used in both simulations. A particle mesh approximation to the Ewald sum (PME) with "tin foil" boundary conditions is used to evaluate the Coulombic interactions.[27] A smooth real space cutoff is applied between 10 and 12 Å, and the Ewald splitting parameter is 0.34 $Å^{-1}$. A grid spacing of approximately 1 Å and a sixth-order interpolation scheme of the charge to the grid are used in the PME. The same cutoff scheme is used for the Lennard-Jones potential, and a long-range correction to the energy and pressure from the Lennard-Jones potential is included.[26]

Membrane polymerization was conducted at constant volume and temperature via a Langevin thermostat (constant volume and temperature, NVT),[26] using a cubic unit cell (unit cell length = 48.7 Å) and an elevated temperature of 340 K. An orthogonal box of pure water was constructed with dimensions matching the *X*,*Y* Cartesian coordinates that are in accord with the membrane and an extended dimension of 136 Å along the *Z* coordinate. This pure water system is equilibrated for 2 ns at 300 K in the NVT ensemble. The final configuration in the last stage of the process of membrane polymerization is used to build membrane−water interfaces. To gain better spatial averaging of the polymerized material, three independent systems are built by using each of the three Cartesian axes (*X*, *Y*, *Z*) of the final cubic system as the membrane normal. An overlay of the membrane with the pure water box in which the water molecules overlapping with the membrane are deleted from the system is used to generate the starting configuration of the hydrated membrane; an interatomic distance of less than 2.6 Å between non-hydrogen atoms of water and membrane is used as the criteria for the overlap, consistent with the experimental oxygen−oxygen radial distribution function of liquid water.[28] Simulations of the three water-solvated membrane systems are performed in the constant temperature and pressure (NPT) ensemble using a temperature of 300 K and a pressure of 1 atm. An equilibration period of 1 ns is used before running production MD simulations of 4 ns in length.

4. Results and Discussion

A. Membrane Polymerization. Assembling a plausible atomic model of the polyamide membrane that respects the molecular constraints posed by the chemical topology and excluded volume of the monomer building blocks is a challenging task. In principle, one might be able to obtain such atomic models by realistically simulating the chemical reactions controlling the polymerization process that leads to the formation of the polyamide membrane. However, the polymerization process takes place over seconds,[29] which is prohibitively slow on the time scale of MD simulations. An alternative strategy is to manipulate the evolution of the atomic configurations artificially to generate a reasonable model of the membrane within a practical simulation time. This is the strategy that we have adopted in the present effort. The procedure used to build the membrane polymer is characterized by four stages that are outlined in Section 2. The topology of the amide bonds that make up the growing polymer is summarized in Table 1 and Figure 2, respectively. Table 1 gives the number of amide bonds formed by the constituent monomeric units. In Figure 2, polymer clusters that have formed are characterized according to their size in units of monomer number. In stage 0, the constituent monomers are arranged with random positions and orientations within a unit cell volume chosen to give a polymer density that is consistent with the experiment. At this stage, there are no steric clashes, and all 500 monomers contain zero amide bonds. The system consists of 500 clusters, each the size of a single molecule. Shown in panel 0 of Figure 3 is the resultant molecular configuration consisting of MPD molecules colored red and TMC monomers colored blue.

TABLE 1: Amide Bond Order of the Individual Monomeric Units of the Membrane Polymer at Each Stage of the Polymerization Process

bonding state	stage 0	stage 1	stage 2	stage 3
MPD (0 bond)	250	2	0	0
MPD (1 bond)	0	24	5	5
MPD (2 bond)	0	224	245	245
TMC (0 bond)	250	19	14	0
TMC (1 bond)	0	61	60	60
TMC (2 bond)	0	99	99	99
TMC (3 bond)	0	71	79	79

Using this initial configuration, an MD simulation is conducted with amide bond formation events interspersed at 1 ps intervals. This phase of the process is denoted stage 1. Shown in Figure 4 is the number of bonds formed after each 1 ps cycle over the course of this simulation. As the polymerization progresses, the rate of polymerization decreases, reflecting the fact that the number of pairs of MDP and TMC molecules within the bonding cutoff distance is getting smaller. After 2000 cycles or a total of 2 ns, the frequency of bonding events slows appreciably. As the membrane polymerizes, it increasingly presents a material barrier to the diffusion of potential reactive monomers, which, along with the reduced concentration of reactive sites, slows the reactive process. At this stage of the polymerization assembly, the system consists of various polymeric clusters of moderate size. Shown in Figure 2, the largest cluster contains 66 monomeric units, and 10 clusters contain more than 15 monomeric units. The molecular configuration is illustrated in panel 1 of Figure 3, where individual amide bonds containing clusters are distinguished by color.

To further propagate the polymerization process, a weak biasing potential energy, presented in Section 2, is introduced

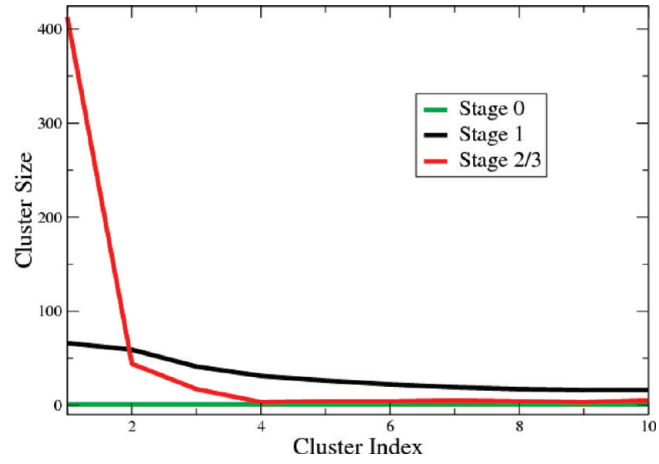

Figure 2. Number of monomers per polymerized cluster at each stage in the membrane assembly. Stage 0 is the initial configuration corresponding to a randomized configuration of monomers without steric clashes. The progression of the membrane polymerization is shown from stages 1−3.

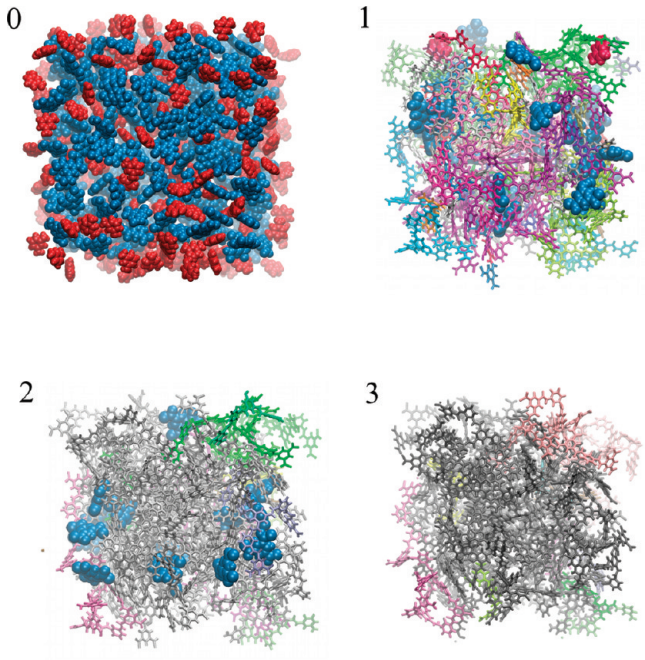

Figure 3. Membrane figures illustrating the four stages of the heuristic membrane build process. Polymerized clusters are distinguished by color. The largest polymer cluster is indicated in gray. Free monomers are represented by van der Waal's surfaces.

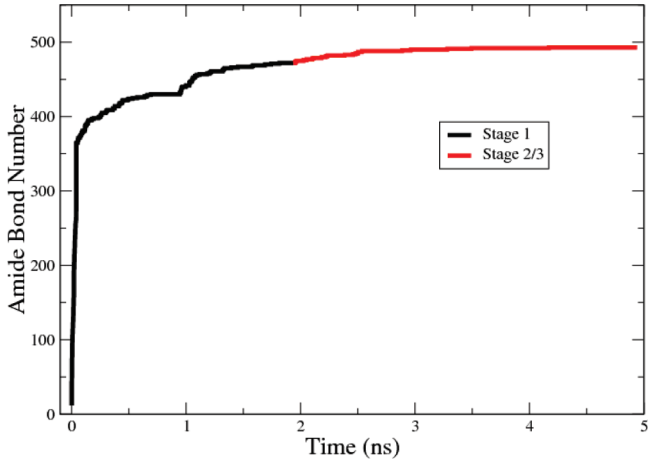

Figure 4. Number of amide bonds formed through the progression of membrane polymer formation.

between bonding partners that are sufficiently near one another. A molecular simulation with this additional potential is conducted in stage 2 in the same manner as in stage 1 with bonding events interspersed at 1 ps intervals. After 3000 cycles or a total of 3 ns, the frequency of bonding events again falls to approximately zero. Shown in panel 2 of Figure 3 is a representation of the molecular configuration of the system. Visible from this representation is a significant change in the amide bond topology of the polymer clusters. The multicolored and varied system of moderately sized clusters has been replaced by a system with fewer distinct clusters with considerably larger size. Shown in Figure 2 is the distribution in monomeric unit size of these clusters. The largest cluster at the end of stage 2 constitutes nearly 80% of the total available monomers, and the number of clusters with greater than 15 monomeric units has fallen to 4. Finally in stage 3 the free acyl chloride monomers are translated to positions near unreacted amine groups, and 500 further cycles of simulation/polymerization are performed before removing the remaining free acyl chloride

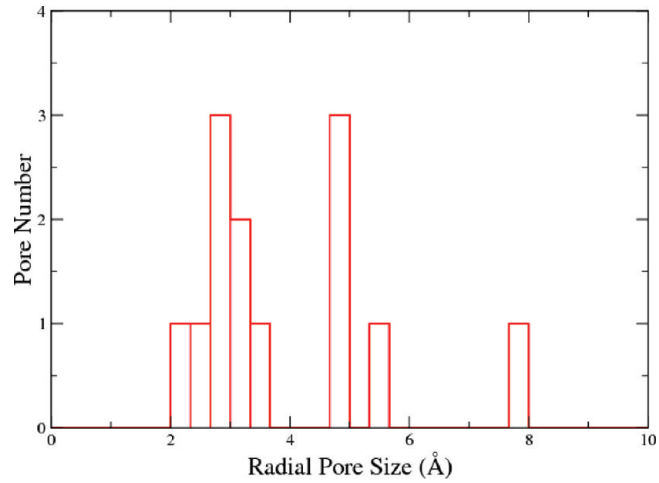

Figure 5. Distribution of free-volume pores in the membrane.

monomers, giving the final polymer membrane topology whose molecular representation is shown in panel 3 of Figure 2.

The distribution of pore size and degree of cross-linking is not controlled directly during the heuristic assembly of the polymerized membrane. Nevertheless, it is of interest to compare them with the results obtained experimentally using PALS.[5] The distribution of free-volume pores, determined from a snapshot of the simulated model membrane, is shown in Figure 5. Presuming a spherical shape, the pore volume is expressed as a radius (R). Two peaks are evident from the figure, corresponding to radii R of approximately 3 and 5 Å. This agrees qualitatively well with PALS experiments, which have identified network pores of ~2 Å and aggregate pores of ~4 Å, for the FT30 membrane. In addition, the ratio of cross-linked to linear segments in the polymer is found to be 37:63 for the model membrane compared to 49:51 determined experimentally.[5]

B. Water Permeability. Experimentally, the permeability of water is determined from a measurement of the water flux through the membrane under a pressure gradient. Assuming linear response holds under the experimental pressure gradient, the flux (J_w) can be determined for the model by employing Fick's law and assuming, on average, a uniform membrane environment,[30]

$$J_w = -D_{mem}K(\Delta C/\Delta Z) \quad (1)$$

where ΔC is the concentration difference across a membrane of width ΔZ. The proportionality constant in eq 1 is a product of the diffusion constant of water in the membrane (D_{mem}) and the water/membrane partition coefficient (K). Furthermore, the experimental difference in pressure can be expressed as a concentration difference using $\Delta C = \rho_w \beta_T \Delta P$ where β_T is the isothermal compressibility of bulk water. To determine the flux of water through the membrane, the membrane diffusion constant and water partition coefficient are determined from equilibrium simulations of the water-solvated polymer membrane.

A pre-equilibrated orthogonal box of pure water is used to solvate the membrane. The membrane can make three interfaces with the orthogonal box of water depending on its orientation. An illustration of one of the membrane−water configurations is shown in Figure 6. The three systems are built and simulated following the procedure outlined in Section 3. Shown in Figure 7 is the concentration profile of water along the membrane normal. It is observed that the water density does not drop sharply at the membrane−bulk interface, reflecting the consider-

Downloaded by UNIV OF CHICAGO on August 27, 2009 | http://pubs.acs.org
Publication Date (Web): July 8, 2009 | doi: 10.1021/jp902715f

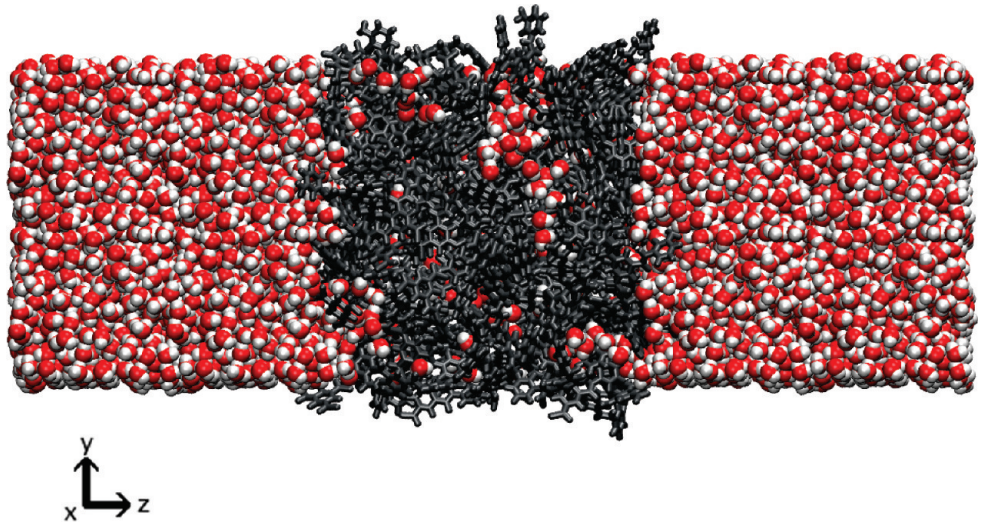

Figure 6. Initial configuration for the simulation of water with the polymer membrane.

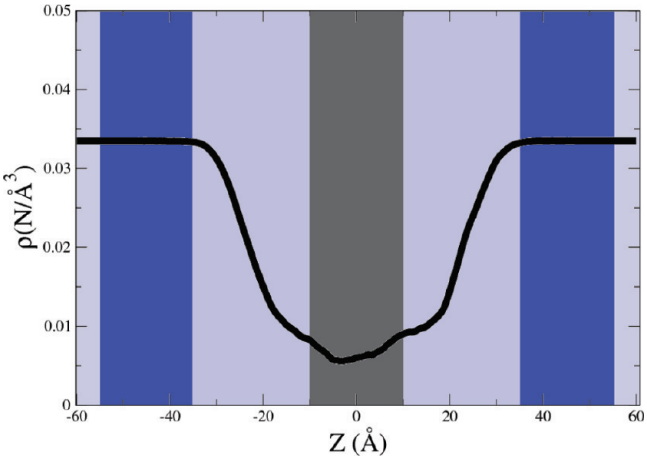

Figure 7. Water molecule density profile along the membrane interface normal. The profile represents an average from the three simulated systems, each taking a different orientation of the polymeric membrane material obtained at the end of stage 3. Bulk water-like regions are shaded dark blue, and the gray region indicates the interior membrane environment.

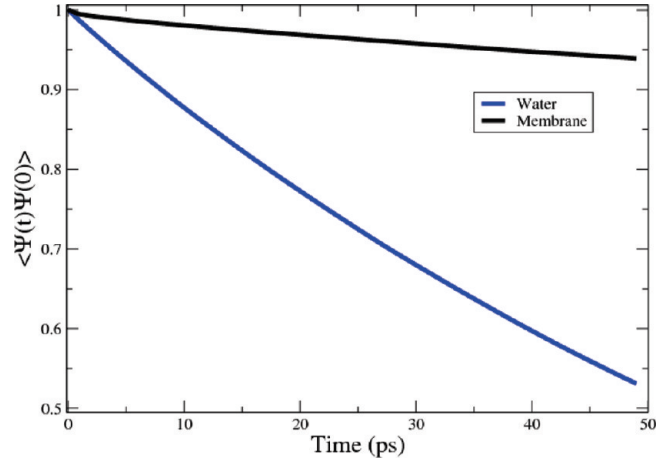

Figure 8. Autocorrelation of the eigenfunction of the diffusion operator under the boundary conditions discussed in Section 4B. The correlation function represents an average from the three simulated systems, each taking a different orientation of the polymeric membrane material obtained at the end of stage 3. The black curve corresponds to the membrane interior shaded gray in Figure 7. The blue curve corresponds to the bulk water regions shaded dark blue in Figure 7.

able porosity of the polymer membrane. To facilitate the analysis, the space is divided into three main regions: bulk water-like regions away from the membrane interface, for $35 < |Z| < 55$ Å, interface regions, for $10 < |Z| < 35$ Å, and a membrane interior region, for $|Z| < 10$ Å. For a membrane with a width in accord with the experiment (0.125 μm), the comparatively small width of the interface regions observed in the simulation (25 Å) should contribute negligibly to the flux of water through the membrane. Rather, the dominant contribution to the flux will arise from the membrane interior region ($|Z| < 10$ Å). In macroscopic measurements, D_{mem} will correspond to the diffusion constant of water within the gray shaded interior membrane region, and the partition coefficient in eq 1 will correspond to the concentration ratio, between bulk water and this region. From Figure 7, the partition coefficient K is determined to be 0.21, which agrees well with the experimental measure of 0.29.[25] In addition, the atomic density in the model membrane interior (1.4 g/cm^3) remains near the experimental water hydrated density of 1.38 g/cm^3.[25]

The diffusive properties of water are expected to vary along the membrane normal reflecting the changing molecular environment. However, we are strictly interested in the diffusion constant within the membrane interior region. To do so, we employ a method that is based on solving the diffusion equation subject to absorbing boundary conditions.[31] The boundary conditions are selected at positions along the normal coordinate that define a spatial region of interest. In the current application we apply planar absorbing boundaries at $Z = -10$ and $Z = 10$ so as to define the interior membrane diffusion constant. The autocorrelation of the resultant eigenfunction of the diffusion operator is related to the diffusion constant by,

$$\langle \psi_n(Z(t))\psi_n(Z(0))\rangle_{\{a,b\}} = (1/L)\exp(-(n\pi L)^2 D_{zz} t) \quad (2)$$

where the eigenfunction $\psi_n(Z) = (2/L)^{1/2}\sin(n\pi(Z-a)/L)$, n is an integer, and $L = b - a$ where b and a are the positions of the boundaries. The subscript $\{a,b\}$ denotes an average over the set of water molecules that stay within the layer between $Z = b$ and $Z = a$ during the time interval t.

As a consistency check, we apply this method to the bulk water regions for $35 < |Z| < 55$ Å shaded dark blue in Figure 7. The decay of the $n = 1$ autocorrelation function is shown in Figure

Downloaded by UNIV OF CHICAGO on August 27, 2009 | http://pubs.acs.org
Publication Date (Web): July 8, 2009 | doi: 10.1021/jp902715f

8. Fitting a single exponential to this curve gives a diffusion constant of 5.1×10^{-5} cm^2/s, which is consistent with the diffusion constant for the TIP3 water model.[32] The autocorrelation function for the interior membrane region for $|Z| < 10$ Å is also shown in Figure 8. The decay is slower than the bulk water curve, and a fit to the exponential in eq 2 gives a D_{mem} diffusion constant of 0.5×10^{-5} cm^2/s.

A recent experiment has measured the water flux per unit density to be 7.7×10^{-6} m/s for a pressure difference of 3 MPa and a membrane thickness of 0.125 μm.[29] The experimental value corresponds to a membrane that is polymerized from an approximately 1:1 molar ratio of constituent reactants. Using the isothermal compressibility of water (4.5×10^{-4} MPa^{-1} at $T = 300$ K) to get ΔC for this experimental pressure difference, along with $\Delta Z = 0.125$ μm and values for K and D_{mem} determined from the simulated data, we get a water flux of 1.4×10^{-6} m/s, which is in fair agreement with the experimental value.

5. Conclusion

To the author's best knowledge, the proposed MD-based method for building all-atom structures of polymeric thin-film materials provides the most realistic atomistic model of the separation layer of RO membranes currently available. This method attempts to capture the inhomogeneous polymerization events that give rise to the complex chemical structure and morphology of these materials. As is thought to occur during the interfacial polymerization process, by which RO membrane thin films are synthesized, the polymeric material generated in this study evolves at the molecular scale as continuously emerging and growing microscopic particles that then aggregate and cross-link to form a dense, inhomogeneous material. Future improvements of the modeling strategy will aim at modulating the evolution of the system during the various stages to control the size distribution of the pores and the cross-linking statistics. The agreement between membrane permeability data calculated by the current simulation and available experimental data (with the same order of magnitude) is very encouraging and suggests that further insight will be gained by simulating aqueous salt solutions.

Acknowledgment. This work was supported by the U.S. Department of Energy (DOE), Office of Basic Energy Sciences, under Contract No. DE-AC02-06CH11357 at Argonne National Laboratory. We would like to thank Yun Luo for helpful discussions.

References and Notes

(1) Koros, W. J. Evolving Beyond Thermal Age of Separation Processes: Membranes Can Lead the Way. *AIChE J.* **2004**, *50* (10), 2326–2334.

(2) Noble, R. D.; Agrawal, R. Separations Research Needs of the 21st Century. *Ind. Eng. Chem. Res.* **2005**, *44*, 2887–2892.

(3) *FILMTEC Reverse Osmosis Membranes Technical Manual*, Form No. 609−00071−0109; Dow Water Solutions: Midland, MI.

(4) Kwak, S. Y.; Jung, S. G.; Kim, S. H. Structure-Motion-Performance Relationship of Flux-Enhanced Reverse Osmosis (RO) Membranes Composed of Aromatic Polyamide Thin Films. *Environ. Sci. Technol.* **2001**, *35*, 4334–4340.

(5) Kim, S. H.; Kwak, S. Y.; Suzuki, T. Positron Annihilation Spectroscopic Evidence to Demonstrate the Flux-Enhancement Mechanism in Morphology-Controlled Thin-Film-Composite (TFC) Membrane. *Environ. Sci. Technol.* **2005**, *39*, 1764–1770.

(6) Zhang, X.; Cahill, D. G.; Coronell, O.; Marinas, B. J. Absorption of water in the active layer of reverse osmosis membranes. Submitted for publication.

(7) Mizukami, K.; Takaba, H.; Kobayashi, Y.; Oumi, Y.; Belosludov, R. V.; Takami, S.; Kudo, M.; Miyamoto, A. Molecular dynamics calculations of CO_2/N_2 mixture through the NaY type zeolite membrane. *J. Membr. Sci.* **2001**, *188*, 21–28.

(8) June, R. L.; Bell, A. T.; Theodorou, D. N. Molecular dynamics study of methane and xenon in silicalite. *J. Phys. Chem.* **1990**, *94*, 8232–8240.

(9) Takaba, H.; Koshita, R.; Mizukami, K.; Oumi, Y.; Ito, N.; Kubo, M.; Fahmi, A.; Miyamoto, A. Molecular dynamics simulation of iso- and *n*-butane permeations through a ZSM-5 type silicalite membrane. *J. Membr. Sci.* **1997**, *134*, 127–139.

(10) Takaba, H.; Mizukami, K.; Kubo, M.; Stirling, A.; Miyamoto, A. The effect of gas molecule affinities on CO_2 separation from the CO_2/N_2 gas mixture using inorganic membranes as investigated by molecular dynamics simulation. *J. Membr. Sci.* **1996**, *121*, 251–259.

(11) Pohl, P. I.; Heffelfinger, G. S. Massively parallel molecular dynamics simulation of gas permeation across porous silica membranes. *J. Membr. Sci.* **1999**, *155*, 1–7.

(12) Lin, J.; Murad, S. A computer simulation study of the separation of aqueous solutions using thin zeolite membranes. *Mol. Phys.* **2001**, *99*, 1175–1181.

(13) Heuchel, M.; Snurr, R. Q.; Buss, E. Adsorption of CH_4-CF_4 Mixtures in Silicalite: Simulation, Experiment, and Theory. *Langmuir* **1997**, *13* (25), 6795–6804.

(14) Firouzi, M.; Nezhad, K. M.; Tsotsis, T. T.; Sahimi, M. Molecular dynamics simulations of transport and separation of carbon dioxide-alkane mixtures in carbon nanopores. *J. Chem. Phys.* **2004**, *120*, 17.

(15) Firouzi, M.; Nezhad, K. M.; Tsotsis, T. T.; Sahimi, M. Nonequilibrium Molecular Dynamics Simulations of Gas Mixtures in Nanopores. *Phys. Rev. Lett.* **1998**, *80*, 3511–3514.

(16) Corry, B. Designing Carbon Nanotube Membranes for Efficient Water Desalination. *J. Phys. Chem. B* **2008**, *112*, 1427–1434.

(17) Zhu, F.; Schulten, K. Water and Proton Conduction through Carbon Nanotubes as Models for Biological Channels. *Biophys. J.* **2003**, *85*, 236–244.

(18) Kotelyanskii, M. J.; Wagner, N. J.; Paulaitis, M. E. Molecular dynamics simulation study of the mechanisms of water diffusion in a hydrated, amorphous polyamide. *Comput. Theor. Polym. Sci.* **1999**, *9*, 301–306.

(19) Cahill, D. G.; Freger, V.; Kwak, S. Y. Microscopy and Microanalysis of Reverse-Osmosis and Nanofiltration membranes. *MRS Bull.* **2008**, *33*, 27–32.

(20) MacKerell, A. D., Jr.; Brooks, B.; Brooks, C. B., III.; Nilsson, L.; Roux, B.; Won, Y.; Karplus, M. CHARMM: The Energy Function and Its Parameterization with an Overview of the Program. In *Encyclopedia of Computational Chemistry*, Vol. 1; John Wiley & Sons: Chichester, 1998.

(21) Wang, J.; Wolf, R. M.; Caldwell, J. W.; Kollman, P. A.; Case, D. A. Development and testing of a general AMBER force field. *J. Comput. Chem.* **2004**, *25*, 1157–1174.

(22) Wang, J.; Wang, W.; Kollman, P. A.; Case, D. A. Automatic atom type and bond type perception in molecular mechanical calculations. *J. Mol. Graphics Modell.* **2006**, *25*, 247–260.

(23) Jakalian, A.; Jack, D. B.; Bayly, C. L. Fast, efficient generation of high-quality atomic charges. AM1-BCC Model: II. Parameterization and validation. *J. Comput. Chem.* **2002**, *23*, 1623–1641.

(24) Jorgensen, W. L.; Chandrasekhar, J.; Madura, J.; Impey, R. W.; Klein, M. L. Comparison of simple potential functions for simulating liquid water. *J. Chem. Phys.* **1983**, *79*, 926–935.

(25) Mi, B.; Cahill, D. G.; Marinas, B. J. Physico-chemical integrity of nanofiltration/reverse osmosis membranes during characterization by Rutherford backscattering spectrometry. *J. Membr. Sci.* **2007**, *291*, 77–85.

(26) Allen, M. P.; Tildesley, D. J. *Computer Simulation of Liquids*; Oxford University Press, Inc.: New York, 1987.

(27) Essmann, U.; Perera, L.; Berkowitz, M. L.; Darden, T.; Lee, H.; Pedersen, L. G. *J. Chem. Phys.* **1995**, *103*, 8577.

(28) Soper, A. K.; Bruni, F.; Ricci, M. A. *J. Chem. Phys.* **1997**, *106*, 247.

(29) Roh, I. J.; Greenberg, A. R.; Khare, V. P. Synthesis and characterization of interfacially polymerized polyamide thin films. *Desalination* **2006**, *191*, 279–290.

(30) Berendsen, H. J. C.; Marrink, S.-J. Molecular dynamics of water transport through membranes: Water from solvent to solute. *Pure Appl. Chem.* **1993**, *12*, 2513–2520.

(31) Liu, P.; Harder, E.; Berne, B. J. On the Calculation of Diffusion Coefficients in Confined Fluids and Interfaces with an Application to the Liquid-Vapor Interface of Water. *J. Phys. Chem. B* **2004**, *108*, 6595–6602.

(32) Lamoureux, G.; Harder, E.; Vorobyov, I. V.; Roux, B.; MacKerell, A. D., Jr. A polarizable model of water for molecular dynamics simulations of biomolecules. *Chem. Phys. Lett.* **2006**, *418*, 245–249.

JP902715F

Downloaded by UNIV OF CHICAGO on August 27, 2009 | http://pubs.acs.org
Publication Date (Web): July 8, 2009 | doi: 10.1021/jp902715f